CHAPTER 1

Chapter 1A

(a) Synthesis of MCM-41

(b) Loading of amino acids (L-Arginine & Cysteine) and drugs (Aspirin, Captopril and Camptothecin) into MCM-41

(c) Characterizations

J Porous Mater (2017) 24:1105–1115
DOI 10.1007/s10934-016-0351-4

Cysteine and *N*-acetyl cysteine encapsulated mesoporous silica: synthesis, characterization and influence of parameters on in-vitro controlled release

Soyeb Pathan[1] · Priyanka Solanki[1] · Anjali Patel[1]

Published online: 7 January 2017

Abstract Pro-drug, cysteine loaded mesoporous silica materials with hexagonal (MCM-41) and cubic (MCM-48) geometry were synthesized by incipient wetness and soaking technique. The structure and properties of these synthesized materials were investigated by various physico-chemical techniques such as FT-IR, Nitrogen adsorption-desorption, XRD and TEM. An in-vitro release study of cysteine from these synthesized materials in SBF was carried out under stirring as well as static conditions. Effect of synthesis method as well as effect of geometry of carrier on release profile of drugs was also examined. Based on the obtained results for pro-drug, controlled release of real drug, N-acetyl cysteine was also carried out under optimized conditions. Release results shows that N-acetyl cysteine release was found to be more controlled as compare to that of cysteine from both mesoporous carriers. A study on release mechanism and release kinetics was also carried out using Higuchi model and first order release kinetic model.

Keywords MCM-41 · MCM-48 · Cysteine · *N*-acetyl cysteine · Controlled release · Kinetics

Electronic supplementary material The online version of this article (doi:10.1007/s10934-016-0351-4) contains supplementary material, which is available to authorized users.

✉ Anjali Patel
aupatel_chem@yahoo.com

[1] Department of Chemistry, Faculty of Science, The Maharaja Sayajirao University of Baroda, Vadodara, Gujarat 390002, India

1 Introduction

The construction of controlled-release systems for targeted drug delivery is of crucial importance for the development of both fundamental science and clinical medicine. In search of optimum drug delivery systems, variety of materials such as polymers [1], polymer based composites, bioactive glasses or ceramics [2, 3] has been frequently investigated. However, traditional disadvantage associated with mentioned systems i.e. disparate distribution of drug through these matrices, are clearly satisfied by mesoporous silica materials (M41S) as they possess ordered mesopores, high surface area, and well defined structure [4–7]. Studies also revealed that M41S have found potential applications for encapsulating bioactive molecules [8–11] and in domain of M41S family, extensive work has been carried out on MCM-41 as drug delivery carrier [12]. Among different bioactive molecules, release studies of ibuprofen from unfunctionalized and/or functionalized MCM-41 have been explored widely [13–19]. In spite of these, release of other molecules such as bisphosphonate [20], cytochrome C [21], cisplatin [22], Sulfadiazine [23], nifedipine [24], amino acids [25] from MCM-41 has also been reported.

The given reports suggested that factors such as the solubility of the drug in the solvent, the diffusivity of the drug in the solvent and the structure characteristics of the pore materials, pore diameter can seriously affect the release behaviors of the drug molecule. It was also shown that one-dimensional (1D) or three-dimensional (3D) cage-like pore structure with of mesoporous silica is of great benefit to control drug release [15]. In spite of these facts, less attention has been paid to other ordered mesoporous silica materials having different geometry e.g. cubic MCM-48 which contains three-dimensional channels. Qiu et al. have studied the release profile of

Materials Science & Engineering C 98 (2019) 1014–1021

Contents lists available at ScienceDirect

Materials Science & Engineering C

journal homepage: www.elsevier.com/locate/msec

Camptothecin encapsulated into functionalized MCM-41: In vitro release study, cytotoxicity and kinetics

Priyanka Solanki[a], Shweta Patel[b], Ranjitsinh Devkar[b], Anjali Patel[a,*]

[a] Department of Chemistry, Faculty of Science, The Maharaja Sayajirao University of Baroda, Vadodara 390002, Gujarat, India
[b] Department of Zoology, Faculty of Science, The Maharaja Sayajirao University of Baroda, Vadodara 390002, Gujarat, India

ARTICLE INFO

Keywords:
MCM-41
12-tungstophosphoric acid
Camptothecin
In vitro release
MTT assay
Kinetics

ABSTRACT

The application of MCM-41 functionalized by 12-tungstophosphoric acid (TPA) as drug carrier for cancer treatment was studied by loading of camptothecin (CPT). In-vitro controlled release study of CPT in Simulated Body Fluid (pH 7.4, 37 °C) was carried out under stirring as well as static conditions. The systems were also evaluated on cancer cells (HepG2) and the carriers are found to be non-toxic to the cancer cells. In order to see the influence of inorganic moiety on release rate of drug, study was also carried out with CPT loaded un-functionalized MCM-41. A detailed study on release kinetics and release mechanism using First Order Release Kinetic Model, Higuchi Model, Koresmeyer-Pepps Model and Extended kinetic model was also carried out.

1. Introduction

Camptothecin (CPT) is a naturally occurring quinolone alkaloid which shows significant anticancer activity with a broad spectrum of human malignancies and CPT is an inhibitor of the DNA-replicating enzyme topoisomerase-I [1]. Unfortunately, the clinical application of CPT is hindered by its poor pharmaceutical profile, with extreme aqueous insolubility, low stability of the lactone form at physiological pH, and severe systemic toxicities which included myelosuppression, vomiting, diarrhoea, and hemorrhagic cystitis [2–4]. A better understanding of mode of action, chemistry and pharmacology of the CPT led to the development of water-soluble derivatives such as irinotecan, topotecan and 9-aminocamptothecin [5]. Although less active than the CPT [6], these derivatives have gained approval by the Food and Drug Administration (FDA) for treating cancers. However, these CPT derivatives still suffer from important drawbacks mainly related to the poor stability of the lactone ring, the short half-life of the compounds in blood and a number of non-resolved toxic effects. Therefore, the development of controlled delivery strategies could lead to significant advantages in the clinical use of these drugs. In this sense, CPT has been encapsulated in different vehicles, like PLGA microspheres [7], solid lipid nanoparticles [8], liposomes [9] and micelles [10]. Reports are also available for camptothecin loading and release using functionalized as well as non-functionalized Silica nanoparticles [11] and polymeric nanoparticles [12]. Further, to modulate the release rate of CPT, carriers are functionalized by various organic molecules such as silica nanoparticles functionalized by 3-Mercaptopropl group [13] and Nucleic acids [14]. Functionalization leads to overcome the mentioned problems faced by CPT.

A literature survey shows that the functionalization was carried out using organic moiety only. It also shows that no reports are found on release study of CPT using either non-functionalized MCM-41 or functionalized MCM-41. In 1992, Mobil Corporation have synthesized the mesoporous silica materials and called as MCM-41. These are amorphous inorganic materials consisting of silicon and oxygen in their framework. Its pore sizes are in range of 2–50 nm in dimension. This material has been widely used as carrier as having unique characteristic such as ordered porosity at the mesoscale, variable pore size, high specific surface area, high adsorption capacity, high concentration of surface Si-OH groups through which it can interact with different functional group of drug. Hence, it was thought of interest to use combination of an inorganic moiety as a functionalizing agent and MCM-41 as new drug delivery systems. The idea was further motivated by recently published result by our group [15] where we have reported functionalisation of MCM-41 (pore diameter: 3.7 nm) by an inorganic moiety, 12-tungstophosphoric acids (TPA) and its use for the in vitro release of L-arginine where we found the beneficial effect of TPA and that encourage us to continue the work.

So, as an extension of our work, for the first time, we describe use of MCM-41 with different pore diameter (4.9 nm) as carrier for CPT. The present article describes functionalization of MCM-41 (pore diameter: 4.9 nm) by TPA, encapsulation of CPT and characterization using

* Corresponding author.
E-mail address: anjali.patel-chem@msubaroda.ac.in (A. Patel).

https://doi.org/10.1016/j.msec.2019.01.065
Received 22 June 2018; Received in revised form 4 January 2019; Accepted 15 January 2019
Available online 16 January 2019
0928-4931/

Experimental

Materials

All chemicals used were of A. R. grade. 12-Tungstophosphoric acid (PW_{12}), sodium hydroxide, Cetyl trimethyl ammonium bromide (CTAB), Tetraethyl orthosilicate (TEOS), n-Hexane, Mesitylene, Ethanol and Sodium hydroxide (NaOH) were used as received from Merck. Ninhydrin, L-Arginine, Cysteine, Aspirin, Captopril and Camptothecin were used as received from Sigma Aldrich.

Synthesis of MCM-41

MCM-41 was synthesized using reported procedure [1] with modification. Surfactant (CTAB, 4.38 g) and NaOH (1.2 g) were dissolved in 200 mL double distilled water. When the solution became homogeneous, TEOS (20.8 g) was added quickly with stirring. After 5 min, mesitylene (8.64 g) and hexane (3.1 g) was added to the stirred mixture. The resulting thick mixture was stirred vigorously for 10 min and then heated at 85 °C for 2 days with stirring. The resulting product was filtered, washed with double distilled water, dried at 100 °C temperature. The obtained material was calcined at 550 °C in air for 5 h and designated as MCM-41 (Figure 1).

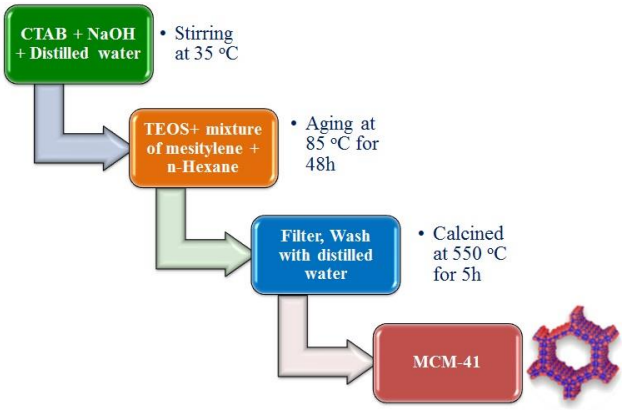

Figure 1. Synthesis of MCM-41

Loading of L-Arginine into MCM-41

Loading of L-Arginine was carried out by incipient wet impregnation method where 1 g of MCM-41 was impregnated with an aqueous solution of L-Arginine (0.1-0.3g/10-30mL). Then mixture was dried at 100 °C for 5 h. The obtained material was designated as L-arg_1/ MCM-41, L-arg_2/MCM-41 and L-arg_3/MCM-41.

Preliminary release study shows that L-arg_2/MCM-41 and L-arg_3/MCM-41 shows burst release. Hence we have selected L-arg_1/MCM-41 for further detailed study and renamed it as L-arg/MCM-41. Preparation of working curve for L-Arginine was not required as loading was carried out by impregnation method.

Loading of Cysteine

Cysteine was loaded over MCM-41 using two different methods (1) soaking method and (2) Incipient wet impregnation method. In the soaking method, 221 mg of MCM-41 was soaked in 10 mL solution of Cysteine (221 mg) in distilled water. The mixture is stirred in sealed vials to prevent the evaporation of solvent for 24 h. Then resulting mixture was filtered and washes with 10 mL of distilled water and dried at room temperature. The obtained material is designated as Cys-MCM-41. The loading amount of Cysteine was obtained by analyzing the filtrate using UV–Vis spectroscopy as well as by TGA.

In incipient wet impregnation method, 1 g of MCM-41 was impregnated with an aqueous solution of Cysteine (0.15 g in 15 mL of distilled water) and dried at 100 °C for 5 h. The obtained material (15 wt% Cys on MCM-41) was designated as Cys-MCM-41(I).

Preliminary release study shows that more controlled and delayed release rate was obtained for the Cys-MCM-41 compared to Cys-MCM-41(I). Hence, further loading of Cysteine was carried out using soaking method only.

Preparation of calibration curve for determination of Cysteine

Stock solution of Cysteine was prepared by dissolving 1 g of it in 100 mL distilled water (10 mg/mL). Series of 10 mL Nessler's tubes containing 0.2 to 0.8 mL of this stock solution was diluted up to the 4 mL using distilled water. 1 mL of acetate buffer (pH 5.5) and 1 mL ninhydrin reagent (10 % ninhydrin solution in ethanol) was added to these solutions. All the tubes were put in boiling water bath up to 10-15 min for completion of reaction which was seen by the formation of purple colour. The solutions were cooled under tap water and then 1 mL of 50 % (V/V) ethanol was added to each of the solutions and absorbance was taken at 570 nm wavelength as per Beer-Lambert's law using Perkin UV-Visible spectrophotometer (Figure 2).

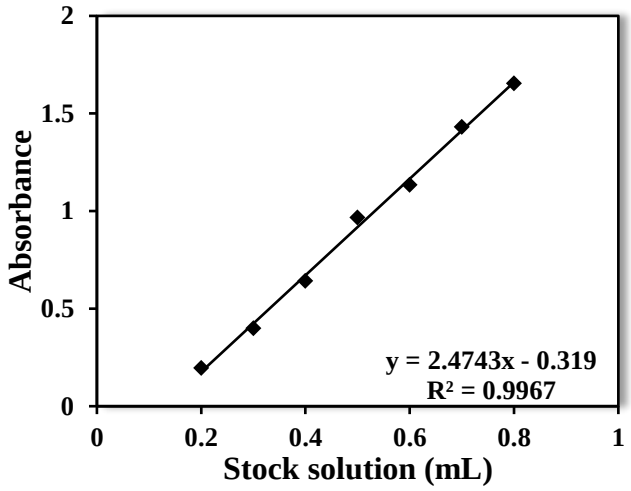

Figure 2. Calibration curve of Cysteine

It is well known that under ideal conditions, Beer-Lambert's law is obeyed when y=mx and c=0. However, in real situations, minor deviations always occur due to various reasons, and in present system they may be caused by variation in path length of radiation across the beam. In order to minimize the errors, the experiment was carried out thrice and error bars were added. This is in good agreement with reported ones [2-8].

Loading of Aspirin, Captopril and Camptothecin

Loading of drugs were also carried out by soaking method. 221 mg of MCM-41 was soaked in 10 mL 0.1 M Aspirin solution in water-ethanol mixture (40:60) mL and stirred for 24 h at room temperature. The sample vials were sealed in order to prevent the evaporation of the solvent. After stirring, the loaded material was filtered through vacuum filtration. The loaded material was washed using 10 mL water-ethanol mixture to remove unbound drug present on surface of MCM-41. The resulting material was air dried and denoted as Asp/MCM-41.

Captopril and Camptothecin were also loaded into MCM-41 using same method and obtained materials were designated as Cap/MCM-41 and CPT/MCM-41. For loading of Camptothecin, dimethylsulphoxide (DMSO) was used as solvent. The amount of drug loading was determined using UV-Visible spectrophotometer by analyzing filtrate at 296 nm, 203 nm and 370 nm for Aspirin, Captopril and Camptothecin respectively.

Preparation of calibration curve for determination of drugs (Aspirin, Captopril and Camptothecin)

Stock solutions of Aspirin, Captopril and Camptothecin were prepared as follows. 10 mg of the drugs were dissolved in 100 mL water ethanol (40:60) mixture (DMSO for Camptothecin). Different concentrations of the drug solutions were prepared (20-240 µg/mL for Aspirin; 10-50 µg/mL for Captopril; 2-18 µg/mL for Camptothecin) by diluting the stock solutions. Absorbance of the solutions was measured using UV-Vis spectrophotometer at 296 nm, 302 nm and 370 nm for Aspirin, Captopril and Camptothecin respectively. The obtained working curves for all drugs were shown in Figure 3. Similar deviations like in case of cys were observed which are attributed to variation in path length and fluorescence (in case of Camptothecin).

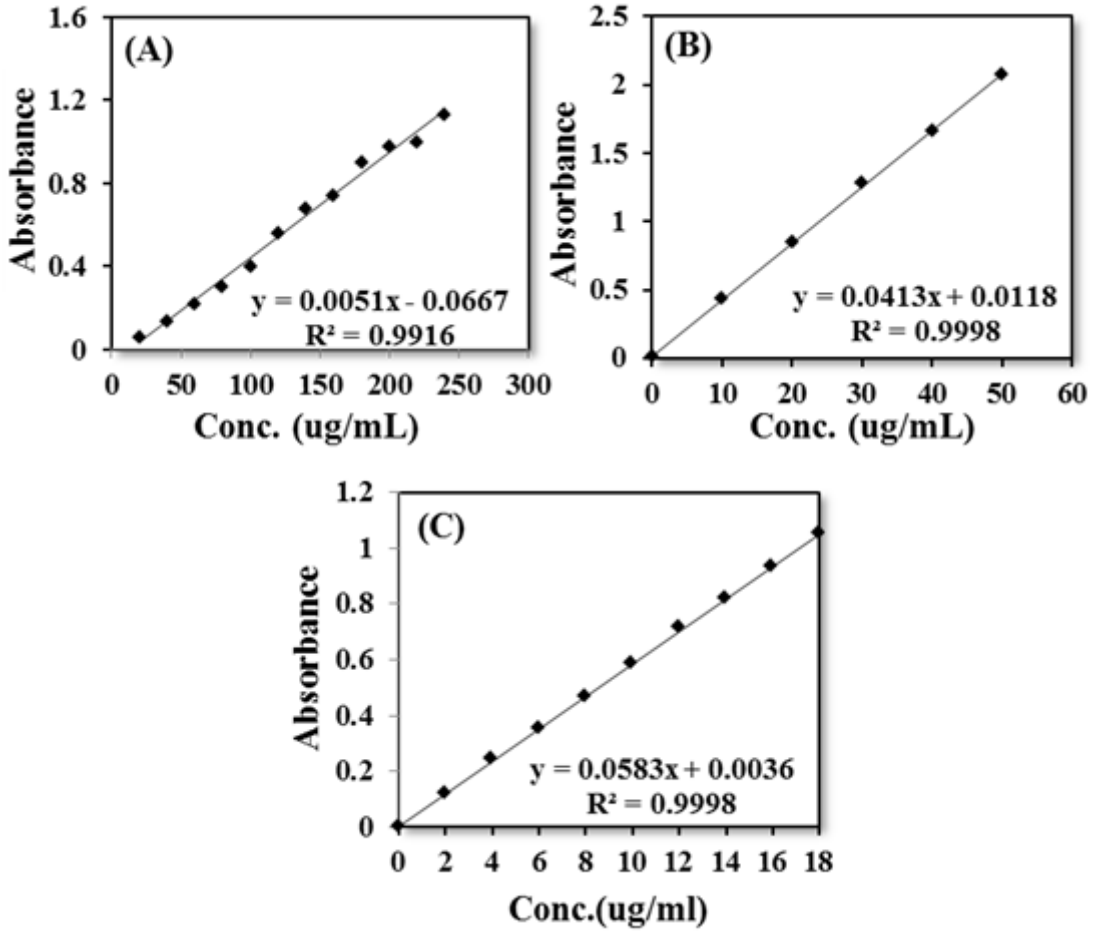

Figure 3. Calibration curve of (A) Aspirin, (B) Captopril and (C) Camptothecin

Characterizations

Characterization is a central aspect of drug carrier development. The elucidation of the structures, compositions, and chemical properties of both the carrier and drugs are very important for a better understanding of the type of interaction between carrier and drug as well as release of drug.

The available analytical techniques can be classified into broad categories based on the information obtained by them.

- Spectroscopic methods which include the study of structural aspects of the drug-carrier.
- Study of surface area, pore volume, pore diameter, particle size distribution, dispersion of the drugs molecules as well as any structural change of drug onto the surface of the carrier.

Spectroscopy is a non-destructive method of analysis and provides information on the types of atoms present on surfaces, how are they influenced by adsorbed species, precise adsorption sites of atoms and molecules, their bond strengths, lengths and angles, and the influence of surface chemical bond on surface reactivity.

In the present chapter, pure carrier and drug loaded carrier were characterized by various physicochemical techniques such as TGA, FT-IR, N_2 adsorption-desorption, XRD, TEM and Solid State ^{31}P MAS NMR. The interaction present between the drug and carrier was predicted from FTIR analysis.

Thermo-Gravimetric Analysis (TGA)

The method in which the effect of heat on the mass of a sample with time is studied to obtain quantitative information is known as the thermo gravimetric method of analysis. There are various parameters which can be obtained from a particular thermal method of analysis namely mass, enthalpy, magnetic properties, and electrical properties. Thermal events are usually recorded by observing the change in the thermal property as the temperature is varied to give a thermal analysis curve or a thermogram.

The thermal events which can lead to some important quantitative information can be melting, phase transition, decomposition, and glass transition. Thermogravimetry, in particular, is the study of the change in mass of the sample as the temperature is varied. When the sample is heated from ambient to 550 °C, under an

atmosphere of O_2 or N_2, characteristic weight losses can be obtained which may yield important information regarding the physical processes occurring in the sample. The magnitude of the weight change can be used to provide the weight change due to that particular transition. When there are more than one process taking place, the thermograms appear to be quite complex, and thus derivative thermograms provide a visual insight to the characteristic weight changes in the sample.

For all the prepared materials, TGA measurements were carried out on the Mettler Toledo Star SW 7.01 in the temperature range 40 ºC to 550 ºC. All measurements were carried out under nitrogen atmosphere with a flow rate of 2 mL/ min and a heating rate of 10 ºC/ min.

Fourier Transform Infrared Spectroscopy (FTIR)

This spectroscopic technique deals with the absorption of electromagnetic radiation in the infra-red region of the electromagnetic spectrum, which probes the changes in the vibrational energy levels of the molecule. This method is widely used in the identification and structural analysis of the organic compounds.

The most common ways of studying an insoluble solid are: 1) as a mull; 2) as a disc; and 3) directly as a powder. These methods differ in terms of degree of difficulty (in obtaining useful spectra), ease of sample preparation, and reliability of the information obtained. Both the mull and disc methods are transmittance techniques. FTIR opaque or highly scattering materials may not be suitable for analysis by transmission spectroscopy.

FTIR absorption spectra of all prepared materials were recorded on a FTIR Perkin Elmer instrument (IRAffinity-1S) at room temperature using KBr pellets in the range of 4000 cm^{-1} to 400 cm^{-1}. The powdered samples were ground with KBr in 1: 10 ratio and pressed (5 ton/cm^2) for making the pellets. The data were collected at an average of 40 scans.

BET measurement

The measurement of the surface area is most important study for the development of any drug delivery systems as surface area may affect the amount of drug loading. For higher surface area shows higher drug loading. Further, from the surface area, one can get the information on the pore volume, pore size which will be helpful to understand the encapsulation of drug.

Apart from surface area measurements, determination of pore size distribution is an equally important parameter as for encapsulation of any drug molecules depend on size of drug as well as pore diameter of carrier. Further, it also affects the release of drug molecules. The standard method for measuring surface areas and pore size are based on the physical adsorption of gas on the solid surface.

Surface area and pore size distribution of all materials were measures according to Brunauer-Emmett-Teller (BET) method, involving nitrogen adsorption-desorption using Micromeritics Surface area Analyzer (Model: ASAP 2020). From the adsorption-desorption isotherms specific surface area was calculated using BET method. The samples were degassed under vacuum (5 – 10.3 mmHg) at 90 °C for 6 h, prior to measurement, to evacuate the physisorbed moisture. Further the pore size distributions were calculated applying the Barrett-Joyner-Halenda (BJH) method to the desorption branches of the isotherm.

Powder X-Ray Diffraction (XRD)

XRD can be used to detect poorly dispersed or macro-crystalline reagent. In principle, XRD can be used to give quick information on the efficiency of dispersion of any drug loaded materials where the drug molecules normally exist in the crystalline state. XRD may also be useful for the identification of any molecules present on the surface of carrier. XRD has also been used to characterize the nature of surface species as well as the structure of carrier before and after drug loading.

The powder X Ray Diffraction pattern of all materials was obtained by using the instrument Philips Diffractometer (Model PW - 1830). The conditions used were Cu K alpha radiation (1.5417 Å), scanning angle from 0° to 10°.

Transmission Electron Microscopy (TEM)

Transmission electron microscopy involves the use of high voltage electron beam which is emitted by the cathode and formed with the help of magnetic lenses. The electron beam which is transmitted from the specimen carries the information about the structure of the specimen. The spatial variation in the image is magnified with a series of magnetic lenses before it hits the detector. The images produced by this type of electron microscopy are two dimensional in nature. Further, it can produce magnification details up to 1,000,000 x with resolution better than $10A^{o}$. The images can be resolved over a fluorescent screen or a photographic film. Furthermore the analysis of the X-ray produced by the interaction between the accelerated electrons with the sample allows determining the elemental composition of the sample with high spatial resolution.

In TEM, the transmission of electron beam is highly dependent on the properties of material being examined. Such properties include density, composition, etc. For example, porous material will allow more electrons to pass through while dense material will allow less. As a result, a specimen with a non-uniform density can be examined by this technique.

TEM was done on JEOL (JAPAN) TEM instrument (model-JEM 100CX II) with accelerating voltage 220 kV. The samples were dispersed in ethanol and ultra-sonicated for 5-10 minutes. A small drop of the sample was then taken in a carbon coated copper grid and dried before viewing.

Solid State MAS NMR (^{31}P)

Nuclear Magnetic Resonance (NMR), since its discovery in 1946, as a technique for the precise determination of magnetic moments of nuclei by physicists has undergone major developments to become one of the most important tools in all branches of science such as chemistry, biology, agriculture and medicine. One can say that it finds applications literally from “molecules to man”. The availability of high field superconducting magnetic has further improved the sensitivity in addition to the resolution. Further developments in the field stem from the introduction of the various multi-pulse techniques which enable the systems to be studied in various phases of

matter viz., liquid, liquid crystalline and solid. The introduction of 2-dimentional techniques is responsible for the study of more complex molecules.

The chemical shift and the coupling constants provide information on the static as well as dynamic properties of molecules. The presence and the absence of the functional groups and their quantitative estimation can be made from the chemical shifts. The coupling constants provide information on the molecular structure and conformation. The function and interaction of the molecules can also be studied by both the chemical shifts and the coupling constants. The chemical exchange, hydrogen bonding and other weak molecular interactions can all be studied by NMR.

In nuclear magnetic resonance**,** magic angle spinning (MAS) is a technique often used to perform experiments in solid-state NMR spectroscopy. By spinning the sample (usually at a frequency of 1 to 70 kHz) at the magic angle θ_m (ca. 54.74°, where $\cos^2\theta_m=1/3$) with respect to the direction of the magnetic field, the normally broad lines become narrower, increasing the resolution for better identification and analysis of the spectrum.

The chemical shifts of peaks in solid state ^{31}P and ^{29}Si NMR spectra were used for characterization of solid materials. The magic-angle spinning (MAS) solid state NMR studies was carried out on a Bruker Avance DSX-300 NMR spectrometer under ambient conditions. The ^{31}P MAS NMR spectra were recorded at 121.48 MHz using a 7 mm rotor probe with 85% phosphoric acid as an external standard. The spinning rate was 4 – 5 kHz. Materials after treatment were kept in a desiccator over P_2O_5 until the NMR measurement. The ^{29}Si NMR spectra were recorded at 121.49 MHz using a 7 mm rotor probe, number of acquisitions AQ: 0.0048888 Sec and spinning rate of 5-7 kHz, with TMS as an external standard.

Results and Discussions

TGA

Figure 4 shows TGA curve of all the materials. TGA curve of MCM-41 shows initial weight loss of 6.14 % at 100 ^{o}C which may be due to the loss of adsorbed water. The final 7.92 % weight loss above 450 ^{o}C may be due to the condensation of silanol groups to form siloxane bonds (Figure 4a). The TGA of L-arg/MCM-41 shows initial weight loss of 7.1% at 100 ^{o}C due to the presence of adsorbed water. Further, weight loss of 10.8% from 200 ^{o}C to 550 ^{o}C suggests the removal of L-Arginine from MCM-41 (Figure 4b). The TGA curve of Cys/MCM-41shows initial weight loss of 1% up to150 ^{o}C which due to the presence of adsorbed water. Further, 15% weight loss from 200 ^{o}C to 550 ^{o}C suggests the removal of Cysteine from MCM-41 (Figure 4c). The TGA curve of Asp/MCM-41 shows initial weight loss of 3.3% due to the loss of adsorbed water up to 150 ^{o}C. Further weight loss of 5.2% from 200 to 550 ^{o}C is may be due to the removal of Aspirin molecules at this temperature. The TGA curve of Cap/MCM-41 shows initial weight loss of 2.3% due to the loss of adsorbed water up to 150 ^{o}C. Further weight loss of 5.2% from 200 to 550 ^{o}C is may be due to the removal of Captopril molecules at this temperature (Figure 4e). The TGA curve of CPT/MCM-41 shows initial weight loss of 42% due to the loss of adsorbed water up to 150 ^{o}C. Further weight loss of 7.3% from 200 to 550 ^{o}C, may be due to the removal of Camptothecin. The amount of drug incorporated into the carrier was also calculated from TGA and data are shown in Table 1.

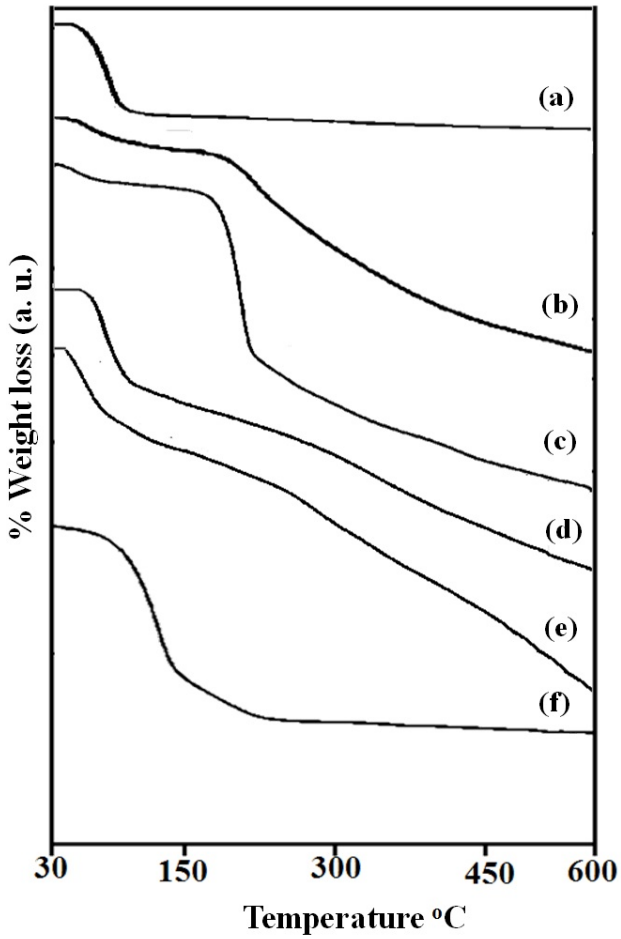

Figure 4. TGA of pure MCM-41, (b) L-arg/MCM-41, (c) Cys/MCM-41, (d) Asp/MCM-41, (e) Cap/MCM-41 and (f) CPT/MCM-41

Table 1. Amount of amino acids/drug loaded into MCM-41

Amino Acid/Drugs	% Loading	Amount of amino acids/drug encapsulated (mg/g of carrier)
L-Arginine	10 ± 0.2	100 ± 2
Cysteine	15 ± 0.2	150 ± 2
Aspirin	5.2 ± 0.2	52 ± 2
Captopril	5.2 ± 0.2	52 ± 2
Camptothecin	7.1 ± 0.2	71 ± 2

FTIR

FTIR bands of MCM-41, L-arg/MCM-41, Cys/MCM-41, Asp/MCM-41, Cap/MCM-41 and CPT/MCM-41 shown in Figure 5. FTIR bands of MCM-41 shows broad band at 1100–1300 cm^{-1}, 3448 cm^{-1} corresponds to asymmetric stretching vibration of Si–O–Si and symmetric stretching vibration of Si–OH group, respectively. The bands at 801 and 498 cm^{-1} represent the symmetric stretching and bending vibration of Si–O–Si. The FTIR bands of L-Arginine shows bands around 3151 cm^{-1}, 1680 cm^{-1}, 1574 cm^{-1} corresponds to N-H stretching vibration, NH_2 in plane bending vibration and C=O stretching vibration which is in good agreement with reported one [9]. The FTIR bands of L-arg/MCM-41 shows additional vibration at 3187 cm^{-1}, 1698 cm^{-1} and 1667 cm^{-1} due to N-H stretching vibration, NH_2 in plane bending vibration and C-O stretching vibration. The band of Si-OH group in L-arg/MCM-41 was shifted to 3364 cm^{-1}. Thus shifting of all bands are observed, however a significant shifting in C-O vibration band (1575 cm^{-1} to 1669 cm^{-1}) and in Si-OH stretching vibration band (3447 cm^{-1} to 3360 cm^{-1}) confirm the interaction between the carbonyl group of L-Arginine and Si-OH group of MCM-41.

The FTIR bands of Cysteine shows typical bands at 3130, 2551, and 1695 cm^{-1} corresponds to NH, SH, and CO respectively. Along with this, 1424 and 1432 cm^{-1}, 1303 cm^{-1}, 1341 cm^{-1} corresponds to CH_2 in plan bending vibration, CH_2 stretching vibration, CH stretching vibration are observed [10]. The FTIR of Cys-MCM-41 shows all the typical bands of MCM-41. In addition, bands correspond to CH_2 stretching vibration (1509 and 1416 cm^{-1}) and CH stretching vibration (1346 cm^{-1}) has been observed. The significant shifting in band of SH group from 2551 to 2361 cm^{-1} indicates the interaction of surface Si-OH group of MCM-41 with SH group of Cysteine.

The FTIR bands of Aspirin shows bands at 1630 cm^{-1}, 3300-3500 cm^{-1},1020-1275 cm^{-1} and 545 cm^{-1} corresponding to C=O, O-H, C-O stretching and CO_2 rocking vibration, in good agreement with reported one [11a, 11b]. The FTIR bands of Asp/MCM-41 shows entire bands related to MCM-41, along with this it shows additional bands at 1638 cm^{-1} and 569 cm^{-1} corresponding to C=O stretching vibration and CO_2 rocking vibration respectively, indicating the presence of Aspirin in the

MCM-41. Shifting in characteristic bands of C=O and CO_2 group in Asp/MCM-41 indicate the interaction of Aspirin through C=O group with carrier.

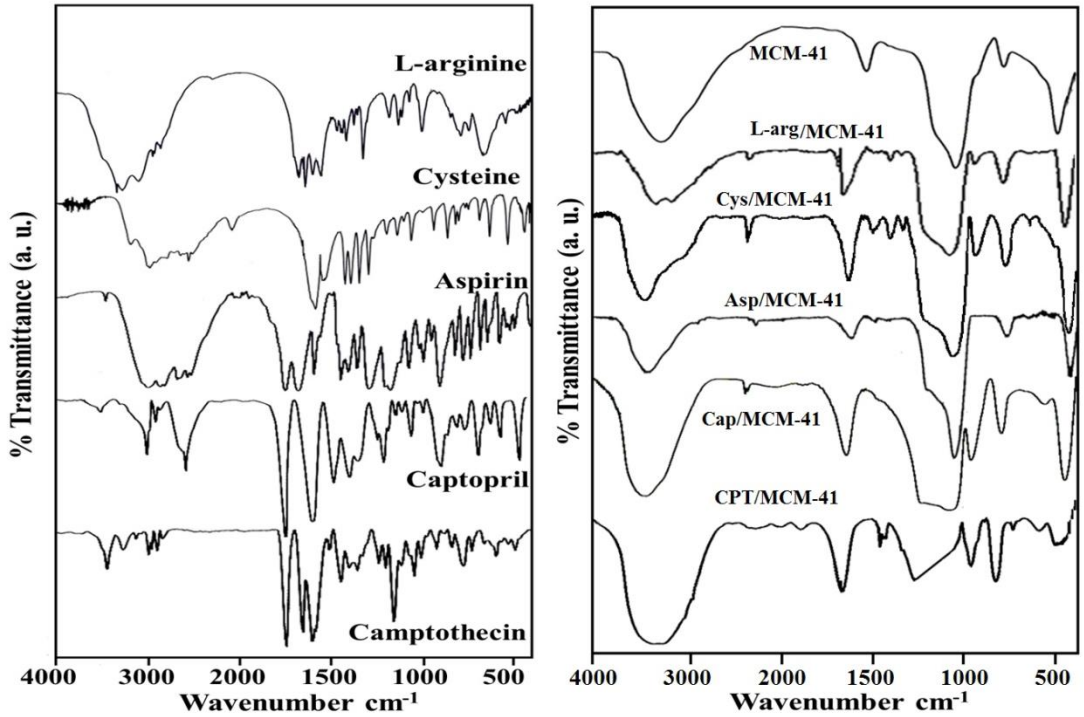

Figure 5. FTIR Spectra of MCM-41, L-arg/MCM-41, Cys/MCM-41, Asp/MCM-41, Cap/MCM-41 and CPT/MCM-41

The FTIR bands of Captopril are observed at 2981 cm^{-1}, 2949 cm^{-1} for CH_3 and CH_2 asymmetric stretching, 2877 cm^{-1} for CH_3, 2567 cm^{-1} for SH, 1747 cm^{-1} for C=O of carboxylic acid, 1469 cm^{-1} for CH_3 bending vibration, 1228 cm^{-1} for C-N stretching vibration [12]. Entire bands related to MCM-41 are present in Cap/MCM-41. Along with this shifting in band of SH and C=O groups are observed from 2567 cm^{-1} to 2363 cm^{-1} and 1747 cm^{-1} to 1637 cm^{-1} respectively. This suggests the interaction of SH and C=O group of Captopril into MCM-41.

The FTIR bands of Camptothecin are observed at 3425 cm^{-1}, 1736 cm^{-1}, 1648 cm^{-1}, and 1436 cm^{-1} corresponding to OH stretching, ester (carbonyl) stretch, carbonyl stretching and C-N stretching vibration, respectively which is in good agreement with reported one [13]. The FTIR Bands of CPT/MCM-41 show entire bands related to MCM-41 indicating intact structure of MCM-41. It also shows bands shifting from 1736 to 1874 cm^{-1} corresponding to Ester (Carbonyl) which indicates the interaction of CPT with MCM-41 through ester carbonyl group.

Nitrogen adsorption-desorption isotherm

Figure 6 shows nitrogen adsorption-desorption isotherms of MCM-41, L-arg/MCM-41, Cys/MCM-41, Asp/MCM41, Cap/MCM-41 as well as CPT/MCM-41 and textural parameters are shown in Table 2. All systems shows type-IV isotherm according to the IUPAC classification with H1 hysteresis loop which is characteristic of mesoporous materials and suggest the intact structure of MCM-41. The surface area of MCM-41 was found to be 890 m^2/g with 1.19 cm^3/g pore volume. Decrease in surface area and pore volume are observed for all the amino acid/drug loaded systems, indicate the insertion of amino acid/drug into the mesoporous channels of MCM-41. However, major decrease in all parameters was observed in case of Cys/MCM-41 compared to rest of the systems. This may be due to the higher loading of Cysteine compared to other systems.

Table 2. Textural properties of materials and amount of drug encapsulated into MCM-41

Materials	**Specific surface area (m^2/g)**	**Pore volume (cm^3/g)**
MCM-41	890	1.19
L-arg/MCM-41	484	0.66
Cys/MCM-41	361	0.48
Asp/MCM-41	764	0.91
Cap/MCM-41	877	0.65
CPT/MCM-41	502	0.55

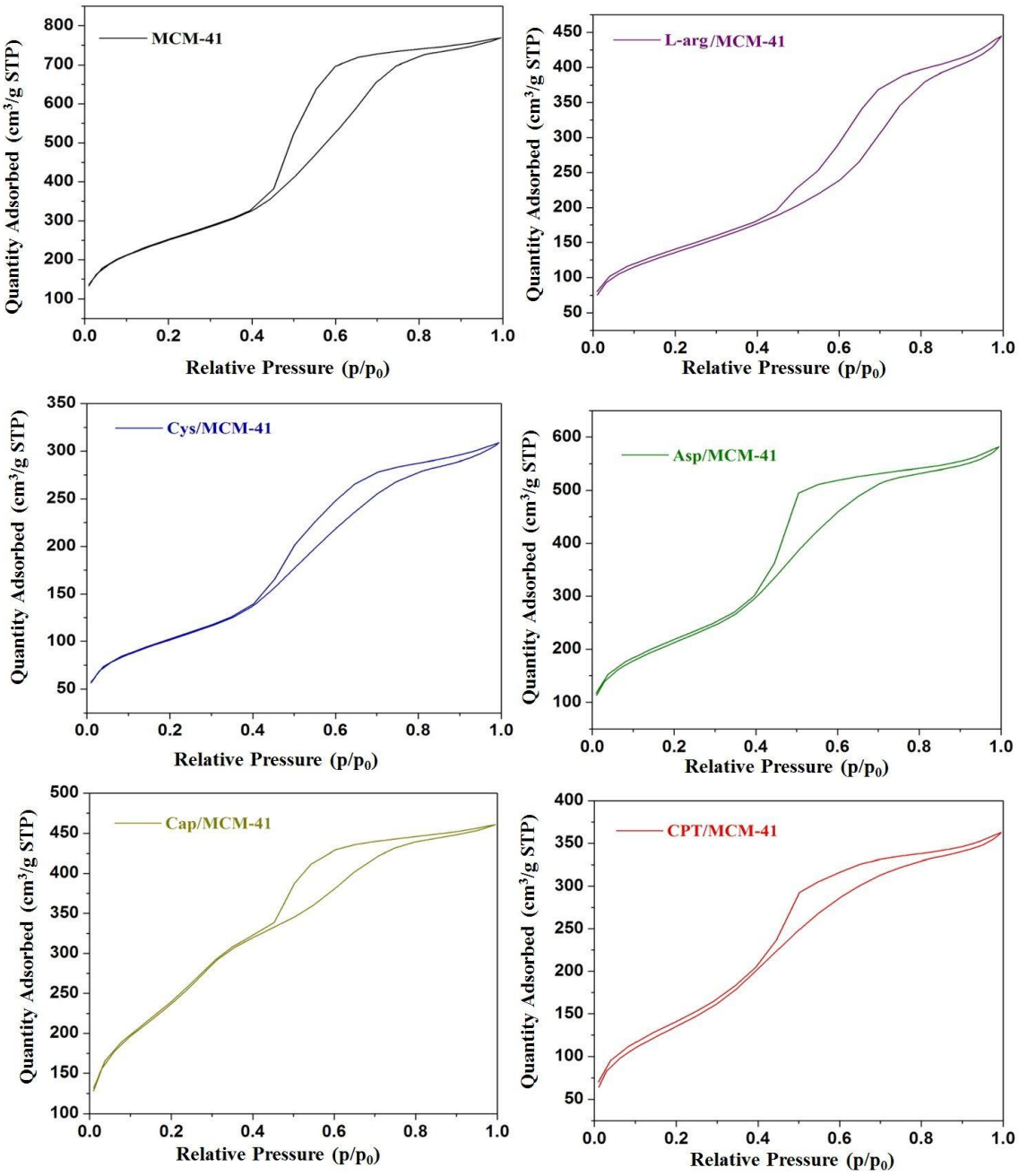

Figure 6. Nitrogen Adsorption-desorption isotherm of all materials

Low angle Powder XRD

Figure 7 Shows low angle powder XRD of all the materials. The low angle XRD of MCM-41 displays an intense diffraction peak at 2θ = 2° which are assigned to the lattice faces (100), suggesting a hexagonal symmetry of MCM-41 (Figure 7a). In addition to this weak peaks are observed at 2θ = 3-5° with very low intensity which are sometimes difficult to observed due to instrumental error [14]. Further, Lu et al have reported similar pattern of XRD peaks of MCM-41 [15]. It is well known that the low angle XRD pattern are sensitive to pore filling and loaded materials show lowered intensity of characteristic peak compared to pure one.

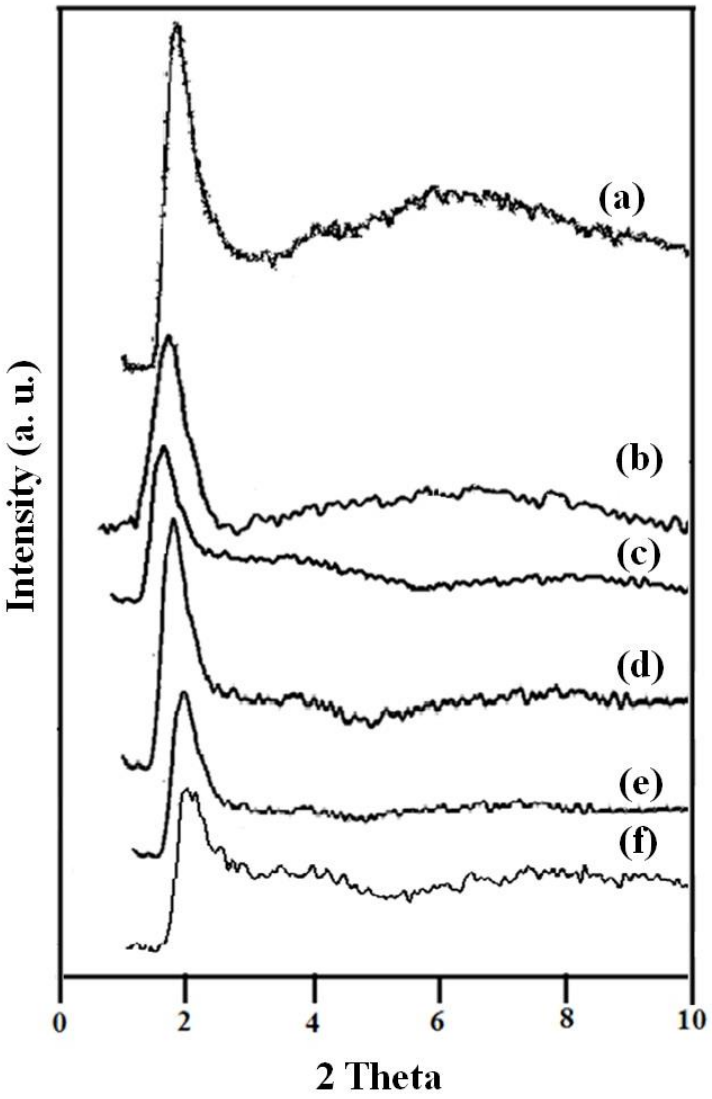

Figure 7 Low angle XRD of (a) MCM-41, (b) L-arg/MCM-41, (c) Cys/MCM-41, (d) Asp/MCM-41, (e) Cap/MCM-41 and (f) CPT/MCM-41.

XRD of L-arg/MCM-41 also shows diffraction peak with lower intensity and slight broadening at 2θ = 2°, suggesting insertion of L-Arginine into mesoporous channels of MCM-41 (Figure 7b).

The XRD pattern of Cys/MCM-41 (Figure 7c) shows shifting in 2θ peak from 2^o to 1.8^o suggests loading of Cysteine to the mesoporous channels of MCM-41. Further, in this case also intensity of diffraction peak is decrease.

The XRD pattern of Asp/MCM-41 also shows characteristics peak at 2θ = 2° with lower intensity suggesting the insertion of Aspirin into the mesoporous channels of carrier which is in good agreement with reported results [16, 17].

The XRD of Cap/MCM-41 and CPT/MCM-41 also shows peak at 2θ = 2° with lower intensity suggesting insertion of Captopril and Camptothecin into mesoporous channels of MCM-41 respectively (Figure 7e and 7f). In all the materials, the structure of MCM-41 remains intact even after loading of amino acids/drugs.

TEM

Figure 8. Shows TEM images of MCM-41, L-arg/MCM-41, Cys/MCM-41, Asp/MCM-41, Cap/MCM-41 and CPT/MCM-41 at 100 nm magnifications. TEM images of MCM-41 shows hexagonal and very well ordered porous structure. TEM image of L-arg/MCM-41 also shows ordered porous structure with absence of any agglomeration suggesting homogeneous distribution of L-Arginine into channals of MCM-41. TEM image of Cys/MCM-41 also shows ordered porous structure with slight darkening as highest loading was observed in same. TEM images of Asp/MCM-41, Cap/MCM-41 and CPT/MCM-41 also shows well-ordered porous structure without disturbing structure of MCM-41.

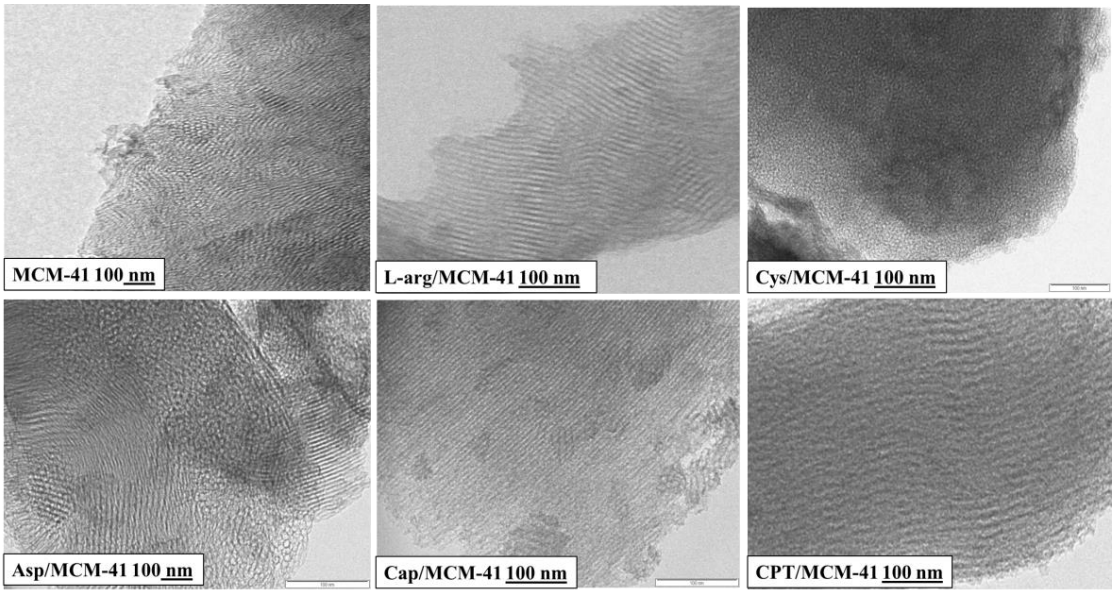

Figure 8. TEM images of MCM-41, L-arg/MCM-41, Cys/MCM-41, Asp/MCM-41, Cap/MCM-41 and CPT/MCM-41 at 100 nm magnifications

Chapter 1B

(a) Functionalization of MCM-41 by 12-tungstophosphoric acid (TPA-MCM-41)

(b) Loading of amino acids (L-Arginine & Cysteine) and drugs (Aspirin, Captopril and Camptothecin) into TPA-MCM-41

(c) Characterizations

Materials

All chemicals used were of A. R. grade. 12-tungstophosphoric acid (TPA), Ethanol, sodium hydroxide (NaOH), NaCl, $NaHCO_3$, KCl, $K_2HPO_4.3H_2O$, $MgCl_2.6H_2O$, HCl, $CaCl_2$, Na_2SO_4 and $NH_2C(CH_2OH)_3$ were used as received from Merck. Ninhydrin, L-Arginine, Cysteine, Aspirin, Captopril and Camptothecin were used as received from Sigma Aldrich.

Functionalization of MCM-41 using 12-tungstophosphoric acid (TPA)

MCM-41 was functionalized using TPA as functionalizing agent by incipient wet impregnation method. 30 % of TPA anchored to MCM-41 was synthesized. 1 g of MCM-41 was impregnated with an aqueous solution of TPA (0.3/30 g/mL of distilled water) and dried at 100 ^oC for 10 h. The obtained material was designated as TPA-MCM-41.

Leaching Test

Whether TPA truly acts as anchoring agent or not, leaching of TPA was investigated. TPA can be qualitatively characterized by the formation of heteropoly blue colour, when treated with a mild reducing agent such as ascorbic acid [18]. In the present study, this method was used for determining the leaching of TPA from the carrier. 1 g of TPA-MCM-41 was stirred in 10 mL water-ethanol mixture (40:60) for 24 h. Then 1mL of the supernatant solution was treated with 10% ascorbic acid. Development of blue colour was not observed, indicating absence of any leaching. The same procedure was repeated with SBF as well SGF, in order to check the presence of any leached TPA. The absence of blue colour indicated no leaching of TPA.

Loading of L-Arginine into TPA-MCM-41

In chapter 1a, we have optimized amount of L-Arginine and hence same amount was further loaded into TPA-MCM-41. Loading of L-Arginine into TPA-MCM-41 was also carried out by same method as described in experimental section of chapter 1a. 1 g of TPA-MCM-41 was impregnated with an aqueous solution of L-Arginine (0.1g/10 mL) and pH of the mixture was adjusted up to 4 using 0.1 M HCl solution and dried at 100 ^oC for 5 h. The obtained material was designated as L-arg/ TPA-MCM-41. Loading

amount was further confirmed by thermal analysis which shows 0.1 g of L-Arginine was loaded per g of TPA-MCM-41.

Loading of Cysteine

Loading of Cysteine into TPA-MCM-41 was also carried out by same, soaking method using same amount of Cysteine as described in experimental section of chapter 1a. The obtained material is designated as Cys/TPA-MCM-41. The loading amount of Cysteine was obtained by analyzing the filtrate using UV–Vis spectroscopy as well as by thermal analysis which shows 8.8% loading of Cysteine into the TPA-MCM-41. This was also calculated by TGA analysis of Cys/TPA-MCM-41.

Loading of Aspirin, Captopril and Camptothecin

Loading of all drugs were also carried out by soaking method as stated in experimental section of chapter 1a. The resulting materials were denoted as Cap/TPA-MCM-41, Asp/TPA-MCM-41 and CPT/TPA-MCM-41. The amount of drug loading was determined by analyzing filtrate at 296 nm, 203 nm and 370 nm respectively and also supported by TGA.

Characterizations

TPA-MCM-41

The synthesized TPA-MCM-41 was characterized by various spectroscopic techniques. Only the main characterization techniques such as EDS, ^{29}Si MAS NMR and ^{31}P MAS NMR are presented here and the rest of the techniques will be discussed along with the amino acids/drug loaded materials.

Results and Discussion

Elemental analysis (EDS)

EDS analysis for TPA-MCM-41 is shown in Table 1. The results obtained from EDS were in good agreement with the theoretical values.

Table 1. Results of elemental analysis in wt%.

Materials	Elemental analysis (weight %)			
	W		P	
	Theoretical	By EDS	Theoretical	By EDS
TPA-MCM-41	19.0	18.0	0.32	0.30

^{29}Si and ^{31}P MAS NMR

Figure 1 shows the ^{29}Si MAS NMR spectra of the MCM-41 and TPA-MCM-41. A broad peak for MCM-41 between -90 and -125 ppm was observed which can be attributed to three main components with chemical shifts at -93, -103, and -110 ppm (Table 2, Figure 1). These signals resulted from Q^2 (-93 ppm), Q^3 (-103 ppm), and Q^4 (-110 ppm) silicon nuclei, where Q^x corresponds to a silicon nuclei with x siloxane linkages, i.e., Q^2 to disilanol Si-(O-Si)$_2$(-O-X)$_2$, where X is H, Q^3 to silanol (X-O)-Si-(O-Si)$_3$, and Q^4 to Si-(O-Si)$_4$ in the framework.

For TPA-MCM-41, all the three bands were observed with broadening and slight shifting which also confirm that the structure of MCM-41 remains intact. A significant shift in Q^2, Q^3 and Q^4 bands are observed which confirm the interaction between surface Si-OH groups to TPA molecules.

Table 2 ^{29}Si chemical shift of MCM-41 and TPA-MCM-41

Materials	^{29}Si MAS NMR data		
	Q^2 ppm	Q^3 ppm	Q^4 ppm
MCM-41	-93	-103	-110
TPA-MCM-41	-89.39	-99.17	-108

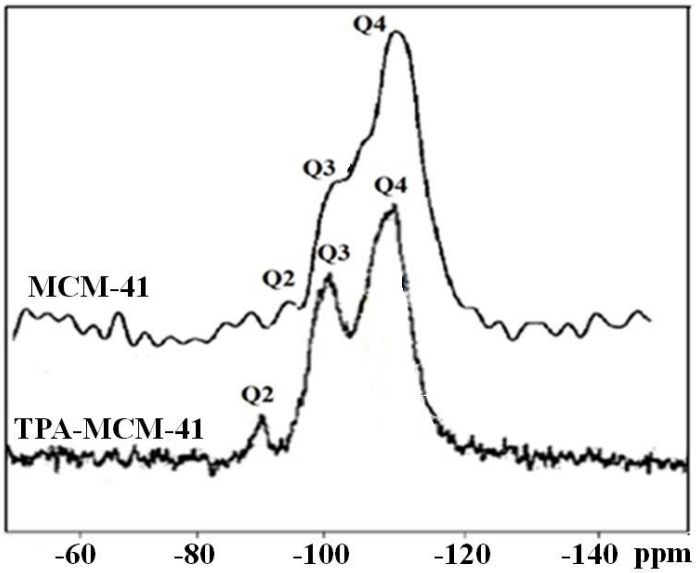

Figure 1. ^{29}Si MAS NMR of MCM-41 and TPA-MCM-41

^{31}P NMR is the most important method to study chemical environment around the phosphorus in heteropoly compounds. The ^{31}P NMR spectra of TPA and TPA-MCM-41 are shown in Figure 2. Pure TPA shows single peak at -15.62 ppm and is in good agreement with the reported one [19]. The ^{31}P NMR spectra of TPA-MCM-41 shows single peak at -12.97 ppm. The observed shift from -15.62 to -12.9 ppm is attributed to the strong interaction of MCM-41 with that of TPA as well as the presence of TPA inside the MCM-41.

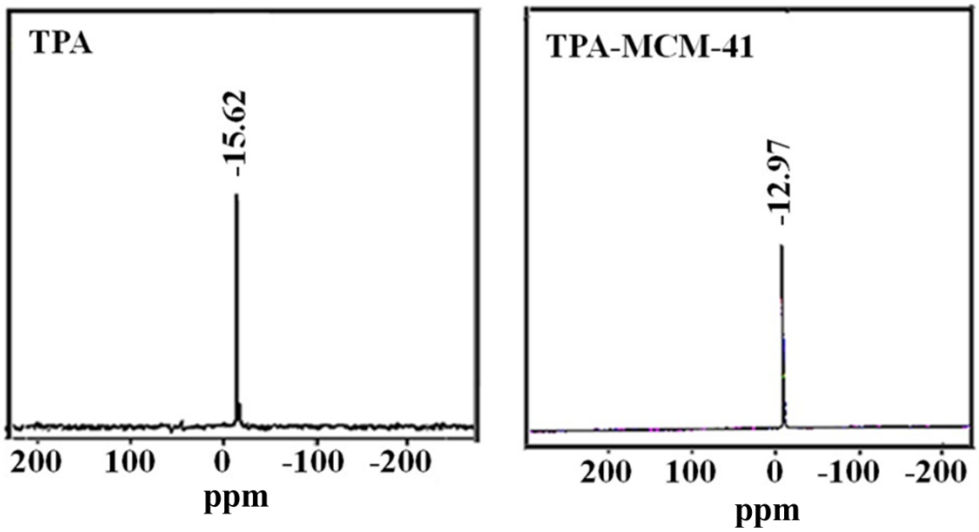

Figure 2. ^{31}P MAS NMR of TPA and TPA-MCM-41

Amino acids/Drug loaded TPA-MCM-41

TGA

TGA of pure TPA, TPA-MCM-41, L-arg/TPA-MCM-41, Cys/TPA-MCM-41, Asp/TPA-MCM-41, Cap/TPA-MCM-41 and CPT/TPA-MCM-41 is shown in Figure 3. TPA exhibits weight loss in three stages at 100, 200 and 485 ^{o}C. These can be attributed to initial weight due to adsorbed water, second weight loss due to loss of water of crystallization near 200 ^{o}C to give the Keggin structure, which is stable on heating up to 350 ^{o}C. The weight loss at 485 ^{o}C may be attributed to the decomposition of the Keggin structure of TPA into the simple oxides [20].

TGA of TPA-MCM-41 (Figure 3b) shows initial weight loss of 3.6 % due to the loss of adsorbed water. Second weight loss of 1.2 % between 150 and 250 ^{o}C corresponds to the loss of water of crystallization of Keggin ion. Further a gradual weight loss was also observed from 250 to 500 ^{o}C due to the difficulty in removal of water contained in TPA molecules inside the channels of MCM-41 [20]. This type of inclusion causes the stabilization of TPA molecules inside the channels of MCM-41.

TGA of L-arg/TPA-MCM-41 shows initial weight loss of 1.76 % due to the loss of adsorbed water. Further weight loss of 10.77 %, from 200 to 450 ^{o}C indicates the removal L-Arginine which also confirms the 10 % loading of L-Arginine into TPA-MCM-41 (0.1 g L-Arginine per g of MCM-41). TGA of Cys/TPA-MCM-41 shows initial weight loss of 2.3 % due to the loss of adsorbed water. Further weight loss of 8.8 %, from 200 to 450 ^{o}C indicates the removal Cysteine which also confirms the 8.8 % loading of Cysteine. The TGA curve of Asp/TPA-MCM-41 shows initial weight loss of 2.4% due to the loss of adsorbed water up to 150 ^{o}C. Further weight loss of 3.8% from 200 to 550 ^{o}C is may be due to the removal of Aspirin molecules at this temperature. The TGA curve of Cap/TPA-MCM-41 shows initial weight loss of 2.6% due to the loss of adsorbed water up to 150 ^{o}C. Further weight loss of 4.9% from 200 to 550 ^{o}C is may be due to the removal of Captopril molecules at this temperature. The TGA curve of CPT/TPA-MCM-41 shows initial weight loss of 19% due to the loss of adsorbed water up to 150 ^{o}C. Further weight loss of 4.9% from 200 to 550 ^{o}C, may be due to the removal of Camptothecin. The amount of amino acids/drugs encapsulated into TPA-MCM-41 is shown in Table 3.

Table 3. Amount of Amino acids/drug Loaded into TPA-MCM-41

Amino Acid/Drugs	% Loading	Amount of amino acids/drug encapsulated (mg/g of carrier)
L-Arginine	10 ± 0.2	100 ± 2
Cysteine	8.8 ± 0.2	88 ± 2
Aspirin	3.8 ± 0.2	38 ± 2
Captopril	4.9 ± 0.2	49 ± 2
Camptothecin	4.9 ± 0.2	49 ± 2

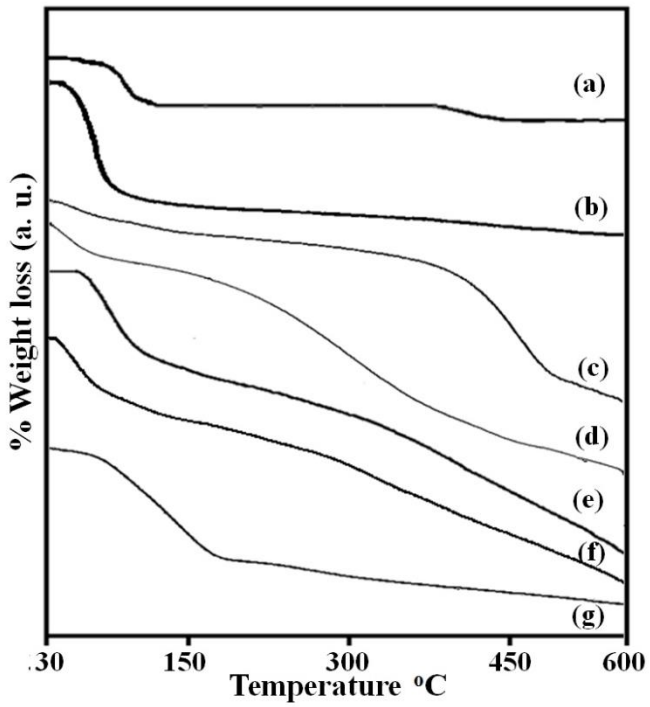

Figure 3. TGA curve of (a) TPA, (b) TPA-MCM-41, (c) L-arg/TPA-MCM-41, (d) Cys/TPA-MCM-41, (e) Asp/TPA-MCM-41, (f) Cap/TPA-MCM-41 and (g) CPT/TPA-MCM-41

FTIR

FTIR bands of TPA-MCM-41, L-arg/TPA-MCM-41, Cys/TPA-MCM-41, Asp/TPA-MCM-41, Cap/TPA-MCM-41 and CPT/TPA-MCM-41 are shown in Figure 4. The reported bands for TPA, at 1088, 987, and 897 cm^{-1} corresponding to P-O stretching, W–O symmetric stretching and W–O-W bending respectively, are absent in TPA-MCM-41. If TPA is dispersed onto the surface of MCM-41, the mentioned bands for TPA should be seen in the FT-IR spectra. The absence of respective FTIR bands of TPA in TPA-MCM-41 may due to the overlapping of TPA bands with that of MCM-41. All the bands of MCM-41 were observed in TPA-MCM-41 which confirms the intact structure of MCM-41.

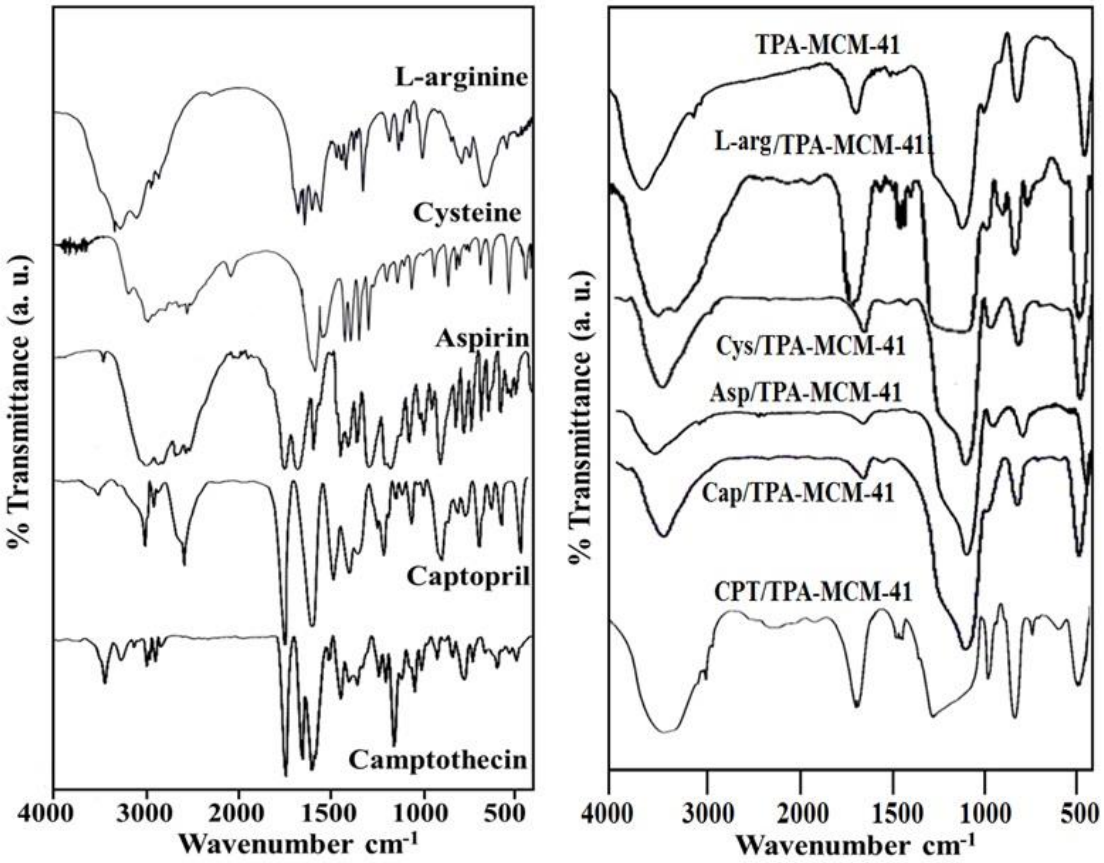

Figure 4. FTIR spectra of TPA-MCM-41, L-arg/TPA-MCM-41, Cys/TPA-MCM-41, Asp/TPA-MCM-41, Cap/TPA-MCM-41 and CPT/TPA-MCM-41

The FTIR of L-arg/TPA-MCM-41 show vibration band with shifting at 3185, 1696 and 1668 cm^{-1}, and due to N–H stretching vibration and NH_2 in plan bending vibration and C=O stretching vibration. Thus shifting of all bands were observed, however significant shifting in N–H stretching vibration (3151–3185

cm^{-1}) and in C=O stretching vibration (1574–1668 cm^{-1}) confirm the strong interaction mainly hydrogen bonding between the N–H and C=O group of L-Arginine and functionalized TPA moiety of TPA-MCM-41.

The FTIR of Cys/TPA-MCM-41 shows entire bands related to TPA-MCM-41. Along with this, it shows additional bands at 1580 and 1404 cm^{-1} corresponding to CH_2 stretching vibration. The significant shifting in band of SH group from 2551 to 2380 cm^{-1} indicates the interaction of Cysteine through SH group.

The FTIR bands of Asp/TPA-MCM-41 show similar bands corresponding in TPA-MCM-41. However, they shows additional bands at 1635 cm^{-1} corresponding to C=O stretching vibration. Shifting in this bands suggest that drug molecules interact with carrier through this C=O group.

The FTIR spectrum of Cap/TPA-MCM-41 also shows same spectrum as that of TPA-MCM-41. Along with this, it shows shifting in band of SH and C=O groups from 2567 cm^{-1} to 2310 cm^{-1} and 1747 cm^{-1} to 1643 cm^{-1} respectively. This suggests the interaction of SH and C=O group of Captopril with TPA-MCM-41.

The FTIR bands of CPT/TPA-MCM-41 shows all the bands related to TPA-MCM-41 and CPT. It also shows shifting in band corresponding to ester carbonyl, from 1736 cm^{-1} to 1884 cm^{-1} which indicate the interaction of CPT with TPA-MCM-41 through C=O group.

Nitrogen adsorption-desorption isotherm

Figure 5 shows Nitrogen adsorption-desorption isotherm of TPA-MCM-41, L-arg/TPA-MCM-41, Cys/TPA-MCM-41, Asp/TPA-MCM-41, Cap/TPA-MCM-41 as well as CPT/TPA-MCM-41 and textural properties of these are shown in Table 4.

The isotherm is type (IV) in nature according to the IUPAC classification and exhibited H1 hysteresis loop which is a characteristic of mesoporous solids for all the six systems. Decrease in all structural parameters of amino acid/drug loaded TPA-MCM-41 suggests the insertion into the porous channels of TPA-MCM-41. Significant decrease in surface area and pore volume is observed in case of L-arg/TPA-MCM-41 as having maximum loading of L-Arginine. In all the case, the basic structure of MCM-41 remains intact. Further, functionalization of MCM-41 by TPA does not alter the structure of MCM-41.

Table 4. Textural properties of materials and amount of drug encapsulated into TPA-MCM-41

Materials	Specific surface area (m^2/g)	Pore volume (cm^3/g)
TPA-MCM-41	622	0.67
L-arg/TPA-MCM-41	180	0.22
Cys/TPA-MCM-41	284	0.35
Asp/TPA-MCM-41	511	0.4
Cap/TPA-MCM-41	337	0.40
CPT/TPA-MCM-41	536	0.56

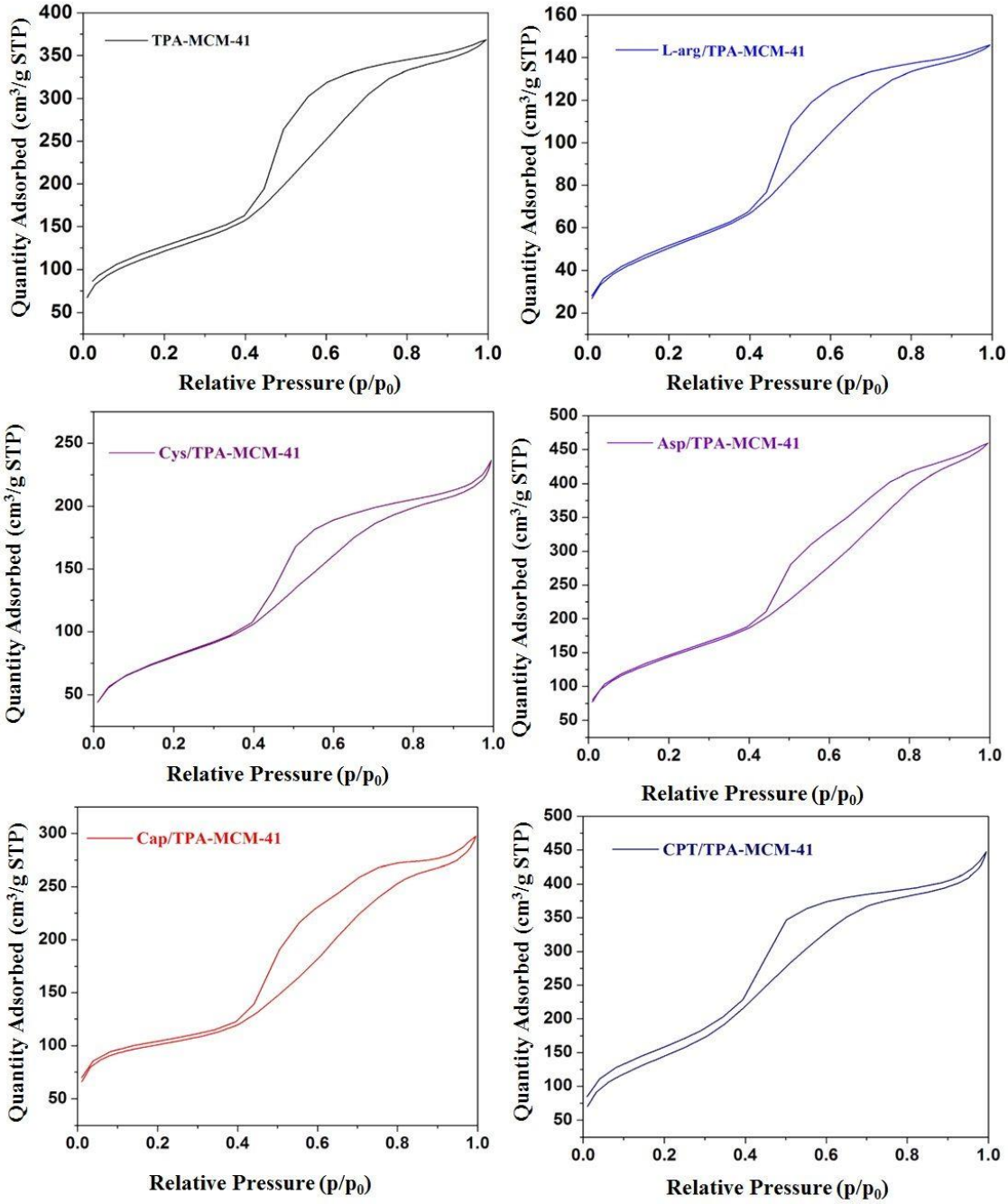

Figure 5. Nitrogen Adsorption-desorption isotherm of all materials

Low Angle Powder XRD

Figure 6 shows low angle powder XRD of (a) TPA-MCM-41, (b) L-arg/TPA-MCM-41, (c) Cys/TPA-MCM-41, (d) Asp/TPA-MCM-41, (e) Cap/TPA-MCM-41 and CPT/TPA-MCM-41. It is well known that the low angle XRD pattern are sensitive to pore filling and loaded materials show lowered intensity of characteristic peak compared to pure one and this reflect in the XRD pattern of all the materials. XRD pattern of all the materials shows characteristics peak at $2\theta = 2°$ with lower intensity. Absence of any other peak indicates the insertion as well as homogeneous distribution of amino acids/drugs into the mesoporous channels of TPA-MCM-41.

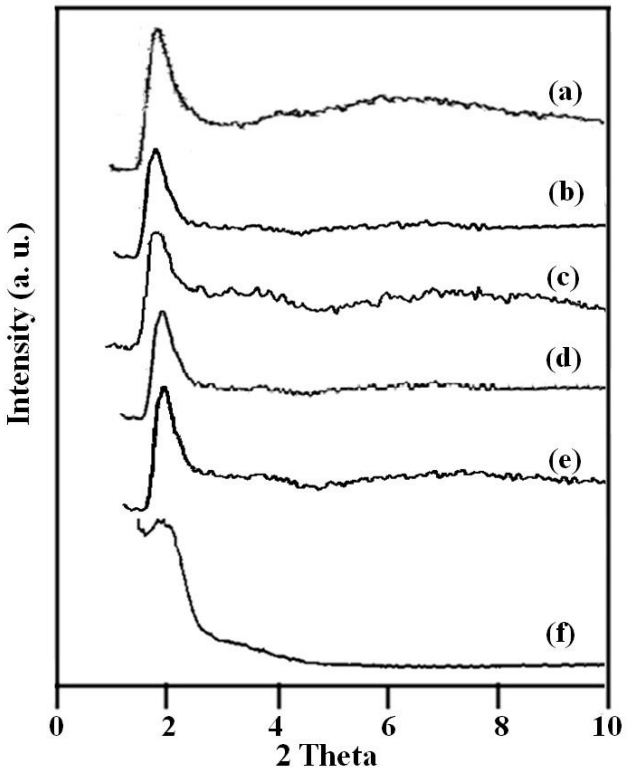

Figure 6. Low angle XRD of (a) TPA-MCM-41, (b) L-arg1/TPA-MCM-41, (c) Cys/TPA-MCM-41, (d) Asp/TPA-MCM-41, (e) Cap/TPA-MCM-41 and (f) CPT/TPA-MCM-41

Further, the structure of MCM-41 remains intact in functionalized as well as drug loaded materials. In addition to this, disappearance of secondary peak at $2\theta = 3\text{-}5°$ in case of amino acid/drug loaded (Figure 6b-6f) was observed. This is because further loading of amino acids/drug into functionalized MCM-41 may block the channels which have already been confirmed by BET analysis. Further the hexagonal mesoporous structure of all the materials are confirmed by TEM (Figure 7).

TEM

Figure 7 Shows TEM images of TPA-MCM-41, L-arg/TPA-MCM-41 Cys/TPA-MCM-41, Asp/TPA-MCM-41, Cap/TPA-MCM-41 and CPT/TPA-MCM-41at 100 nm magnification. TEM images of all show hexagonal and very well ordered porous structure. TEM images of TPA-MCM-41 shows absence of crystalline phase of TPA inside the channels of MCM-41 indicating high dispersion of TPA and absence of agglomeration. TEM images of all materials shows ordered porous structure with absence of any agglomeration indicating the well dispersion of amino acids/drug into TPA-MCM-41.

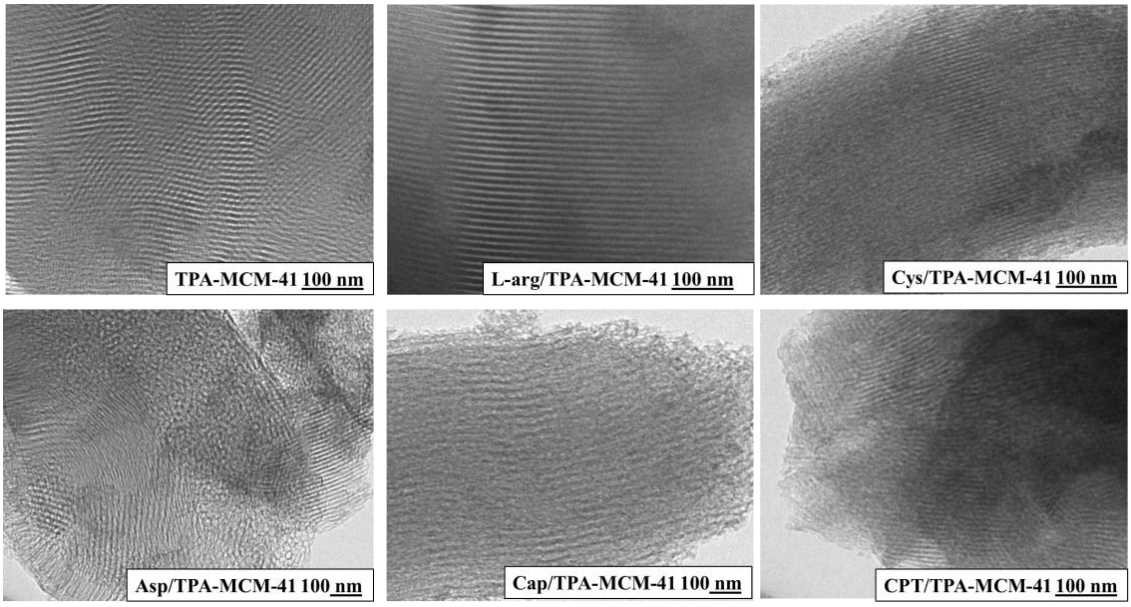

Figure 7. TEM images of TPA-MCM-41, L-arg/TPA-MCM-41, Cys/TPA-MCM-41, Asp/TPA-MCM-41, Cap/TPA-MCM-41 and CPT/TPA-MCM-41

Conclusion

- Synthesis of MCM-41 as well as functionalization was successfully achieved by non-hydrothermal synthetic method and by using wet impregnation method using TPA and confirmed by elemental analysis and spectral studies.
- FTIR shows that TPA interacts with MCM-41 through Si-OH group of MCM-41. Decrease in all parameters of BET surface area shows the insertion of TPA into the mesoporous channels of MCM-41.
- Loading of amino acids/drugs have been successfully achieved by wet impregnation and soaking method.
- FTIR analysis suggests the interaction between amino acids/drugs and carrier (MCM-41, TPA-MCM-41) which is mainly H-bonding.
- BET surface area analysis shows decrease in all parameters for amino acids/drugs loaded carrier which indicates insertion of amino acids/drugs into channels of carrier.
- Low angle powder XRD and TEM analysis show absence of agglomeration and homogeneous dispersion of amino acids/drug into MCM-41 as well as TPA-MCM-41.

References

[1] H. Myong, A. SteinLim, Chem Mater 11, 3285-3295 (1999)

[2] Z. Yasmeen, T. Mamatha*, H. Farheen, H.K Qureshi, Asian J. Pharma. Clini. Res. 6, 2, 164 (2013).

[3] S.A. Hapse, P.T. Kadaskar, A.S. Shirsath, Der Pharmacia Lettre, 3, 6, 18 (2011).

[4] S. Antakli, N. Sarkis, M. Kabaweh, Asian J. Chem. 22, 6, 4931 (2010).

[5] R.S. Joshi, N.S. Pawar, S.S. Katiyar, D.B. Zope, A.T. Shinde, Der Pharm. Sinica,2,3, 164 (2011).

[6] S.U. Jan, G.M. Khan, I. Hussain, Pak. J. Pharm. Sci., 25,751 (2012)

[7] A.R. Mahmood, M. Abdullah, B.T. mohammed; Z.A. Jabbar Conf. Series: Mater. Sci. Eng. 571, 012104 (2019)

[8] R.D Parmar, P. Kapupara, K. Shah, J. Chem. Pharm. Res. 10, 6, 87 (2018)

[9] S. Kumar, S.B. Rai, Indian J. pure appl. Phys. 48, 251 (2010).

[10] A. Patel, V. Brahmkhatri, In: M. Aliofkhazraei (Eds. 2015, vol 3), Comprehensive Guide for Mesoporous Materials, Properties and Development, Nova Science Publishers, Inc., pp. 271-284.

[11] (a) V. Renganayaki, S. Srinivasan, S. Suriya, Int J Chem Tech Res ISSN: 0974-4290, 4, 3 983-990 (2012). (b) I.G. Binev, B.A. Stamboliyska, Y.I. Binev, J. Mol. Struct. 378, 189 (1996).

[12] A.P. Imran, A.G. Nayan, R.R. Bhushan, S.P. Pawar, Int J pharm Sci 4:4, ISSN: 0976 (2013).

[13] A. Patil, S. Patil, S. Mahure, A. Kale, Am. J. Ethno. 1, 3, 174 (2014).

[14] M. Kruk, M. Jaroniec, Langmuir, 15, 5279 (1999).

[15] H.Y. Zhu, X.S. Zhao, G.Q. Lu, D.D. Do, Langmuir, 12, 6513 (1996).

[16] A. Szegedi, M. Popova, I. Goshev, S. Klebert, J. Mihaly, J. Solid State Chem. 194, 257 (2012).

[17] B. Marler, U. Oberhagemann, S. Vortmann, H. Gies, Microporous Materials, 6, 375 (1996).

[18] G.D. Yadav, V.V. Bokade, Appl. Catal. A 147, 299 (1996).

[19] T. Okuhara, N. Mizuno, M. Misono, Adv. Catal. 41, 113 (1996).

[20] G. Kamalakar, K. Komura, Y. Kubota, Y. Sugi, J. Chem. Technol. Biotechnol. 81, 981 (2006).